JACS
JOURNAL OF THE AMERICAN CHEMICAL SOCIETY
Article
pubs.acs.org/JACS

Mercaptocarborane-Capped Gold Nanoparticles: Electron Pools and Ion Traps with Switchable Hydrophilicity

Ana M. Cioran,[†] Ana D. Musteti,[†] Francesc Teixidor,[†] Željka Krpetić,[‡] Ian A. Prior,[§] Qian He,[∥] Christopher J. Kiely,[∥] Mathias Brust,*[,‡] and Clara Viñas*[,†]

[†]Institut de Ciencia de Materials de Barcelona, ICMAB-CSIC, Campus UAB, E-08193 Bellaterra, Spain

[‡]Department of Chemistry, Crown Street, University of Liverpool, Liverpool L69 7ZD, United Kingdom

[§]The Physiological Laboratory, Institute of Translational Research, University of Liverpool, Liverpool L69 3BX, United Kingdom

[∥]Department of Materials Science and Engineering, Lehigh University, 5 East Packer Avenue, Bethlehem, Pennsylvania 18015-3195, United States

Supporting Information

ABSTRACT: A simple single-phase method for the preparation of ca. 2 nm gold nanoparticles capped with mercaptocarborane ligands is introduced. The resultant monolayer protected clusters (MPCs) exhibit redox-dependent solubility and readily phase transfer between water and nonpolar solvents depending on the electronic and ionic charge stored in the metal core and in the ligand shell, respectively. The particles and their properties have been characterized by high angle annular dark field imaging in a scanning transmission electron microscope, elemental analysis, centrifugal particle sizing, UV−vis and FTIR spectroscopy, and thermogravimetric analysis and by ^{1}H, ^{11}B, and ^{7}Li NMR spectroscopy. Cellular uptake of the MPCs by HeLa cells has been studied by TEM, and the subsequent generation of reactive oxygen species inside the cells has been evaluated by confocal fluorescence microscopy. These MPCs qualitatively showed significant toxicity and the ability to penetrate into most cell compartments with a strong tendency of finally residing inside membranes. Applications in catalysis, electrocatalysis, and biomedicine are envisaged.

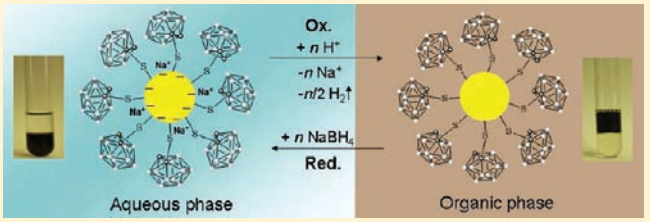

INTRODUCTION

Thiolate-stabilized gold nanoparticles, now commonly referred to as monolayer protected clusters (MPCs), have been studied with unabated enthusiasm since the initial report of a simple two-phase liquid/liquid protocol in 1994, which enabled the gram scale preparation of dodecanethiolate-capped particles in the 1.5 to 4 nm size range that were stable under ambient conditions as isolated solids and readily redispersible in nonpolar solvents.[1] Owing to this unprecedented stability and the ease of preparation, MPCs of gold and, to a much lesser extent, silver were rapidly adopted by researchers across discipline boundaries and soon facilitated a number of important studies of typical nanoscale phenomena that had hitherto been virtually inaccessible to experimental investigation. These include electrochemical quantized capacitance charging,[2] room temperature Coulomb blockades,[3] activated electron hopping conductivity in nanoparticle solids and thin films,[4] self-organization of nanocrystal superlattices,[5] reversible metal−insulator transitions,[6] and NMR spectroscopy of self-assembled monolayer thin films,[7] to name only a few.

The practical importance of MPCs is evidenced, for example, by their current role in the development of artificial nose-type gas sensors with potential applications in lung cancer diagnostics based on breath analysis.[8] The first crystal structure of a typical representative of this class of materials stabilized by mercaptobenzoic acid (MBA), $Au_{102}MBA_{44}$, was published in 2007,[9] and others followed,[10] generally suggesting that the stability of the clusters stems partly from their electronic closed shell structure[11] as previously observed in series of alkali metal clusters with so-called magic numbers of electrons.[12] Recently, much MPC work has focused on the use of water-soluble clusters for biomedical applications, such as drug and gene delivery and photodynamic therapy.[13] Hydrophilic thiols successfully used as capping agents for this purpose include sugars,[14] peptides,[15] polymetacrylate,[16] and polyethylene glycol (PEG) derivatives.[17] Solubility is a general problem that often poses limits to the chemical versatility of MPCs, which, in principle, could be prepared with any combination of chemical and/or biomolecular functionalities in the ligand shell. In practice, many ligand shell modifications compromise the particles' colloidal stability and cause aggregation.

While the chemical properties of MPCs are dominated by those of the functional groups present in the ligand shell, it is well established that the metal core can accept or donate a number of electrons in discrete steps, as evidenced by electrochemical charging experiments.[2] At the cathodic limit this leads, under certain conditions, to the destabilization of the particles

Received: April 20, 2011
Published: December 3, 2011

   dx.doi.org/10.1021/ja203367h | J. Am. Chem.Soc. 2012, 134, 212−221

by reductive loss of thiolate ligands.[18] The vast majority of electrochemical experiments with MPCs, beginning with Murray's pioneering work that introduced the concept of quantized capacitance charging, have been carried out in non-aqueous media using MPCs stabilized by short chain alkanethiols to enable electron transfer across the ligand shell.[2] The compared to water low dielectric constants of such media implies low double layer capacitances and hence allows the observation of single electron charging steps at the expense of limiting the amount of charge that can be stored on each cluster. In water, colloidal metals acting effectively as electron pools have been known for some time and were first reported by Henglein and co-workers,[19] but charge-dependent transfer of metallic particles across the water/oil interface has not been observed in any system reported to date.

Here we introduce a single-phase route to a new type of MPC, which is hydrophobic and completely insoluble in water when uncharged, but, when offered electrons by a suitable reducing agent, transfers readily to an aqueous phase where it behaves as a Henglein-type electron pool. In addition, exchangeable cations can be stored in the ligand shell. When discharged, the particles precipitate in water and redissolve readily in less polar solvents. These unprecedented properties are due to the use of mercaptocarborane clusters as capping agents, which, like other thiol ligands, effectively stabilize the gold core, but owing to their spherical shape necessarily leave gaps that allow direct access of reactants and solvent molecules to the gold surface. The design of water-soluble boron rich macromolecules or particles is of significance for Boron Neutron Capture Therapy (BNCT) and for drug delivery.

Ortho-carborane, 1,2-*closo*-$C_2B_{10}H_{12}$, nearly retains the perfect icosahedral geometry of the parent borane after substitution of two adjacent boron atoms with two carbons.[20] It is chemically and thermally extremely stable but, like its derivatives, highly hydrophobic and generates water-insoluble structures with limited bioavailability and hence is unsuitable for application in BNCT.[21] The excellent water-solubility of the materials prepared here is thus highly unusual, representing a rare case of a carborane-based macromolecular unit with potentially high bioavailability.

We have characterized these new MPCs by TEM, scanning transmission electron microscopy-high-angle annular dark field (STEM-HAADF), UV−vis, infrared, and NMR spectroscopy, centrifugal particle sizing (CPS), thermogravimetric analysis (TGA), and quantitative analysis of boron, gold, and sulfur by X-ray photoelectron spectroscopy (XPS), and atomic emission spectroscopy (AES), and we describe in detail their unusual redox-switchable hydrophilicity as well as ion exchange phenomena. To illustrate potential biomedical applications of their unique solubility characteristics, we have demonstrated the cellular uptake of these MPCs from aqueous solution by a human cancer cell line and show that the particles penetrate membrane structures as they are oxidized and become more hydrophobic within the biological environment. It is also been shown that uptake of these MPCs causes significant stress by the generation of reactive oxygen species (ROS). We believe that these new materials offer a broad scope for exciting research and future applications.

EXPERIMENTAL SECTION

Materials. Chlorauric acid and *tetra*octylammonium bromide were purchased from Sigma Aldrich, 1-octanethiol from Fluka, and sodium borohydrate from Katchem. All chemicals were used as purchased. Diethyl ether, acetone, methanol, and hydrochloric acid were purchased from Carlo Erba-SdS, and isopropanol was obtained from VWR BDH PROLABO. Mercaptocarborane,1-SH-1,2-*closo*-$C_2B_{10}H_{11}$, was synthesized according to the literature.[22]

Methods. *Preparation of Mercaptocarborane-Capped MPCs.* 50 mg of mercaptocarborane (0.283 mmol) and 111 mg of chlorauric acid (0.283 mmol) dissolved in 60 mL of methanol and 64 mg of sodium borohydride (1.6998 mmol) dissolved in 30 mL of methanol were added immediately under vigorous stirring. The mixture was stirred at room temperature for 10 min before the solvent was removed by rotary evaporation. The dark-brown residue was first thoroughly washed with diethyl ether to remove excess mercaptocarborane and then dissolved in isopropanol and filtered to remove the remaining sodium borohydride and other insoluble contaminants. After rotary evaporation of the isopropanol, the final product was obtained as a dark-brown solid. IR (NaCl): ν = 3063 (s, ν_{C-H}), 2584 (v s, ν_{B-H}). ^{1}H NMR (300 MHz, CD_3COCD_3, $Si(CH_3)_4$) δ (ppm): 3.48 (s, 1H, C_c−H), 3.00−1.50 (m, 10H, B−H). ^{1}H{^{11}B} NMR (300 MHz, CD_3COCD_3, $Si(CH_3)_4$) δ (ppm): 3.48 (s, 1H, C_c−H), 2.81 (br s, B−H), 2.59 (br s, B−H), 2.21 (br s, B−H), 1.80 (br s, B−H). ^{11}B NMR (96 MHz, CD_3COCD_3, $BF_3{\cdot}Et_2O$) δ (ppm): −1.86 (d, ^1J(B−H) = 143 Hz), −7.09 (d, ^1J(B−H) = 170 Hz), −8.92 (d, ^1J(B−H) = 147 Hz), −11.69 (d, ^1J(B−H) = 166 Hz).

Infrared. Spectra of MPCs were recorded on a NaCl plate after evaporation of a drop of MPCs dispersed in acetone using a Perkin-Elmer Spectrum One spectrophotometer, which covers a wavelength range from 4000 to 400 cm^{-1}. UV−vis spectroscopy was carried out with a Shimadzu UV−vis 1700 spectrophotometer at 23 °C using 1 cm quartz cuvettes. ^{1}H and ^{1}H{^{11}B} NMR (300.13 MHz) and ^{11}B and ^{11}B{^{1}H} NMR (96.29 MHz) spectra were recorded with a Bruker ARX 300 instrument equipped with the appropriate decoupling accessories. Chemical shift values for ^{11}B NMR spectra were referenced to external $BF_3 \leftarrow OEt_2$, ^{7}Li NMR spectra were referenced to 1 M LiCl aqueous solution and those for ^{1}H and ^{1}H{^{11}B} NMR spectra were referenced to $SiMe_4$. Chemical shifts are reported in units of parts per million downfield from reference and all coupling constants in Hz.

XPS. Experiments were performed in a PHI 5500 Multitechnique System (from Physical Electronics) with a monochromatic X-ray source (Aluminum Kalfa line of 1486.6 eV energy and 350 W), placed perpendicular to the analyzer axis, and calibrated using the 3d5/2 line of Ag with a full width at half-maximum (fwhm) of 0.8 eV. The analyzed area was a circle of 0.8 mm diameter, and the selected resolution for the spectra was 187.5 eV of pass energy and 0.8 eV/step for the general spectra and 23.5 eV of pass energy and 0.1 eV/step for the spectra of the different elements. All measurements were made in an ultra-high vacuum (UHV) chamber pressure between 5×10^{-9} and 2×10^{-8} Torr. Quantitative analysis of Au and B by atomic emission spectroscopy was carried out using a Spectro Ciros ICP-AES spectrometer.

Particle Imaging and Sizing by STEM. TEM specimens were prepared by allowing one drop of the diluted ethanolic sol to evaporate on a lacey carbon film supported by 300 mesh copper grid. STEM-HAADF images of nanoparticles were obtained in order to determine the metal dispersion using a JEOL 2200FS transmission electron microscope equipped with a CEOS probe corrector. A 30 mm condenser aperture (~25 mrad) and a probe current of ~60 pA were used when acquiring the images. The particle size distribution was determined by measuring the 2D projected area of nearly 2000 particles. Particle diameters were derived by assuming all the particles are ideal spheres.

Particle Sizing by Analytical Centrifugation. Particle size and distribution was estimated using a CPS disc centrifuge DC24000 (CPS Instruments Inc.). For measurements, the speed was set to 24 000 rpm, and the centrifuge disc was successively filled with a density gradient liquid (8−24% w/w sucrose dissolved in Milli-Q water) leaving it to stabilize for 1 h prior to analysis. The disc was filled successively in nine steps, starting with the dilution of highest density. Prior to analysis of the nanoparticles, calibration was performed using as a calibration standard 0.377 μm PVC particles (Analytik Ltd.). All nanoparticle samples were sonicated before injection in the disc

centrifuge. The size of the particles was calculated using CPS Software (9.5c) for the density of 6.5 g cm^{-3}.

TGA. Analysis was performed for a 1.32 mg sample in a Al_2O_3 crucible, using a NETZSCH STA 449F1 Jupiter thermogravimetric analyzer under an argon atmosphere at 10 K min^{-1} heating rate from 313.15 to 673.15 K. The Argon flow rate was of 60 mL min^{-1}. Proteus software was used for the measurement and evaluation of the resulting data.

MPC Phase Transfer Experiments. Phase transfer of MPCs from water to diethyl ether has been carried out in two different ways: (i) irreversibly, with the phase transfer agent *tetra*octylammonium bromide, and (ii) reversibly, by acidification of the aqueous phase with dilute hydrochloric acid. For (i) a test tube was filled with ca. 4 mL of the aqueous dispersion of MPCs and the same volume of diethyl ether to give a two-phase system. Solid *tetra*octylammonium bromide was added in small portions under regular shaking until all MPCs had transferred to the ether phase. A movie of this experiment is shown in Supporting Information. For (ii), instead of adding a phase transfer agent, the aqueous phase was acidified by addition of a small volume of dilute hydrochloric acid, which led to the formation of a few gas bubbles (presumably hydrogen) and transfer of MPCs to the ether phase. Photos of this experiment are shown in Scheme 2. Once the ether phase contained the MPCs, the acidified aqueous phase was replaced by a freshly prepared aqueous solution of sodium borohydride, which led to the re-extraction of the particles back into the aqueous phase.

Cellular Uptake of Nanoparticles and Cell Imaging by Electron Microscopy. HeLa cells were incubated for 2 h with MPCs dispersed in cell culture medium. After incubation the excess of nanoparticles was removed, and cells were rinsed twice with 2 mL of warmed PBS (1×) buffer. Subsequently, the cells were fixed by addition of 4% paraformaldehyde/2.5% glutaraldehyde in phosphate buffer (0.7 mL) for 1 h. Then the cells were rinsed with PBS buffer, postfixed using 1% aqueous solution of OsO_4 (0.5 mL) for 1 h (caution! extremely toxic). Subsequently the cells were washed with Milli-Q water, 30% ethanol solution and stained with 0.5% uranyl acetate (0.5 mL, in 30% ethanol) for 1 h. Cells were then gradually dehydrated using a series of ethanol solutions (30, 60, 70, 80, and 100%) and embedded in epoxy resin. The resin was polymerized at 60 °C for 48 h. Ultrathin sections (70–100 nm) were cut using a diamond knife on a Leica Ultramicrotome and mounted on Formvar-coated copper grids. The sections were then poststained using 5% uranyl acetate in 50% ethanol and 2% aqueous lead citrate solution and imaged with FEI Tecnai Spirit TEM at 100 kV using AnalySIS software (Soft Imaging Systems).

Detection of Reactive Oxygen Species (ROS) and Confocal Microscopy. Confocal microscopy was carried out to detect ROS production in the cells incubated for 30 min with mercaptocarborane-capped MPCs using the ImageiT Live detection kit (Molecular Probes, Invitrogen detection technologies). Cells were cultured in 35 mm glass-bottom dishes (Iwaki, Asahi Techno Glass, Tokyo, Japan), and fluorescence was measured using a Zeiss LSM510 microscope (Jena, Germany) with a 63 plan apochromatic oil immersion objective (NA = 1.4). The intracellular ROS levels were detected using 5-(and-6)-carboxy-2′,7′-dichlorodihydrofluorescein diacetate (carboxy-H_2DCFDA). Carboxy-H_2DCFDA is a nonfluorescent cell-permeable indicator for ROS that becomes fluorescent upon oxidation by ROS after cleavage of the protecting acetate groups by intracellular esterases. After incubation with the nanoparticles, the cell culture medium was replaced with fresh complete medium in the presence of 25 mM of carboxy-H_2DCFDA. After 20 min incubation at 37 °C, the dye was washed twice with complete medium, and intracellular fluorescence was detected using an argon ion laser at 488 nm for excitation and a 505–550 nm bandpass filter from a 545 nm dichroic mirror for emission. Data capture was performed with LSM510 version 3 software (Carl Zeiss GmbH, Jena, Germany).

RESULTS AND DISCUSSION

Preparation and Properties and a Structural Model for Redox Switchable Solubility. The single-phase reaction leading to mercaptocarborane-capped gold nanoparticles with a mean total diameter of 3.2 nm (determined by CPS) is schematically illustrated in Scheme 1.

Scheme 1. Formation of Au Nanoparticles

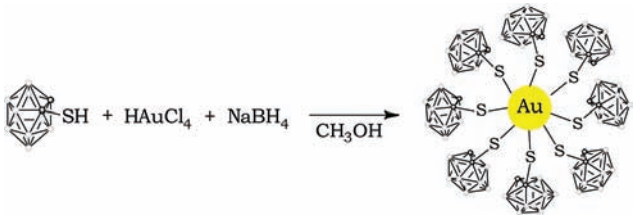

The mercaptocarborane used here has been successfully employed before by Base et al. both for the modification of flat gold electrodes and the preparation of MPCs of comparable size.[23] Their particles were very thoroughly characterized but did not show unexpected or unusual properties in comparison with MPCs stabilized by more conventional thiolate ligands. The reason for this is that the authors had followed the traditional two-phase liquid/liquid route, which requires the use of *tetra*octylammonium bromide as a phase transfer agent.[23] As a result, *tetra*octylammonium ions formed part of the product, which then no longer exhibits the remarkable electron and ion storage abilities and the switchable solubility behavior we wish to report here. Kennedy et al. attached mercaptoborane to 25 nm aqueous silver colloids to devise a delivery system for boron neutron capture therapy and reported strong Raman enhancement of the B–H stretching mode but did not further characterize the material.[24] STM studies of self-assembled monolayers (SAMs) of mercaptocarborane on macroscopic gold[23] and silver[25] surfaces have been reported.

The modified method we report here features a number of characteristics during the preparation step that are worth being highlighted and discussed along with some peculiar observations of the particles' solubility behavior, since this provides important intuitive chemical insight into this complex nanosystem. The preparative protocol is very simple and basically consists of the addition of sodium borohydride to a methanolic solution of chlorauric acid in the presence of the mercaptocarborane. While in previously reported single- and biphasic preparations of MPCs any excess of borohydride appears to be tolerated, this system here is very sensitive to the amount of borohydride added, so that once a threshold of approximately 7-fold stoichiometric excess with respect to Au(III) reduction is reached, the clear brown solution of nanoparticles turns abruptly into a black slurry followed by irreversible precipitation of the entire gold content as a black powder. Also as a purified product, our particles remain prone to decomposition in the presence of a large amount of borohydride. While this obviously has to be avoided, this property indicates that unlike other MPCs, these are amenable to further reduction by borohydride and eventually suffer reductive loss of the protective thiolate ligands, which has previously only been observed in electrochemical experiments using MPCs capped with hexanethiol.[18] We attribute this to the necessary openness of the ligand shell resulting from the fact that it is impossible to cover a sphere (Au core) with smaller spheres (carboranes) without leaving gaps and to the very small diameter of the carborane of about 0.5 nm, which may still allow electron transfer from borohydride to the gold core across the ligand shell. Given the size of the carborane, the gaps will not be narrower

than 0.25 nm, even at closest packing of carborane spheres, and thus will permit most ions and small molecules direct access to the gold surface.

Once the particles have been prepared, the solvent, methanol, is removed to yield the dry crude product still containing excess ligands, sodium borohydride, and any possible byproduct. Curiously, the resultant solid dissolves not only in alcohols and acetone but also in water, while it is insoluble in diethyl ether and less polar solvents. MPCs consisting only of a gold core and a shell of mercaptocarborane ligands should be very hydrophobic and hence completely insoluble in water. Their solubility in polar solvents therefore is a very surprising finding. Nevertheless, once dissolved in water, the particles can be readily extracted into diethyl ether by addition of the phase transfer agent *tetra*octyammonium bromide to the organic phase. This quantitative extraction shown in the movie (see Supporting Information) demonstrates unequivocally the net anionic character of the particles when present in the aqueous phase. Once *tetra*octylammonium ions are added, the process is irreversible, and the particles will no longer be soluble in water. In fact, it was impossible to separate the particles from the phase transfer agent, which appeared to have become an integral part of the ligand shell. MPCs treated in this way are probably very similar to those previously reported by Base et al.[23] The perhaps more interesting reversible transfer of the particles from water to diethyl ether is achieved by acidification of the aqueous phase with dilute hydrochloric acid. Upon addition of the acid, the particles precipitate from the aqueous phase under evolution of a small amount of gas, presumably hydrogen (also in the absence of borohydride), and redissolve readily in the organic phase. In a two-phase system direct extraction from the aqueous to the organic phase is observed. Re-extracting the particles into an aqueous phase is possible by addition of sodium borohydride but cannot be achieved simply by an alkaline aqueous phase. This demonstrates that it is not an acid–base reaction but a redox reaction that switches the solubility of the particles. The process is completely reversible, and the same particles can be isolated as a solid, redissolved, and moved back and forth between diethyl ether and water phases without any evidence of aging effects. An interesting observation is the formation of relatively stable water/diethyl ether emulsions and even gels during these experiments. They are likely to be Pickering emulsions stabilized by particles at the interphase between the two immiscible liquids. These emulsions are readily broken up by the addition of a few drops of acetone.

Based on our extensive experience with MPCs and summarizing all indicative observations detailed above, a simple model that describes the particles as both electron and ion storage devices is presented in Scheme 2. It is proposed that the readily accessible gold core acts as an electron pool that is in Nernstian equilibrium with its surrounding electrolyte solution.

In the presence of sodium borohydride, the core charges up negatively by storing a number of excess electrons, which are counter balanced by sodium ions occupying the voids between the carborane spheres on the surface of the particle and presumably also within the electrochemical double layer depending on the amount of charge that needs to be balanced. The cathodic limit of this charge storage process is the observed decomposition of the material by reductive desorption of ligands, for example, after addition of excess borohydride. This structural model also explains the observed anionic behavior of the particles. As illustrated in Scheme 3, the dissociation of sodium ions from the core leads to the formation of giant polyanions, which can be extracted into nonpolar solvents with *tetra*octylammonium bromide, as shown. Positive charging of the core by reaction with suitable oxidizing agents has not been attempted but should be an interesting goal of future work along with a full electrochemical characterization of these materials.

Scheme 3. Formation of Giant Polyanions

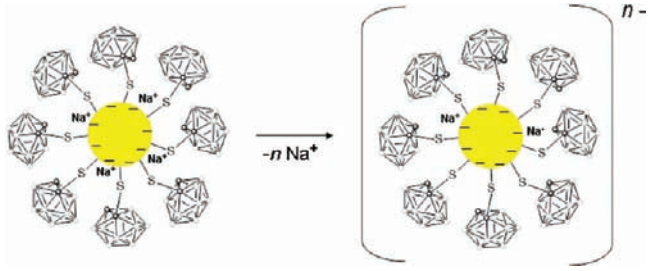

The stored electrons are removed from the gold core by mild oxidation in dilute acid under evolution of hydrogen, as also shown in Scheme 2. Concurrently, sodium ions desorb, and the

Scheme 2. Model Illustrating the Particles Both As Electron and Ion Storage Devices

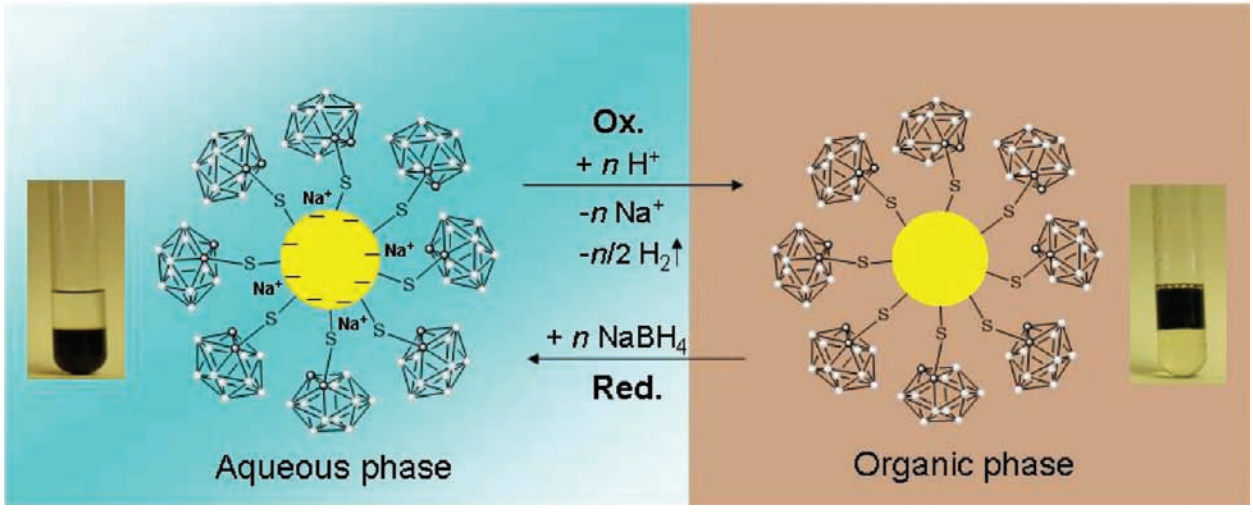

dx.doi.org/10.1021/ja203367h | J. Am. Chem.Soc. 2012, 134, 212–221

particles become much less hydrophilic and either precipitate or transfer to the organic phase if present. Finally, a simple experiment was conducted in order to demonstrate that the voids between the carboranes could be irreversibly filled by a suitable molecular stopper, here octanethiol. A day after addition of a small amount of octanethiol to a solution of MPCs in diethyl ether it was no longer possible to transfer the particles to water by addition of borohydride. Also, the particles were now tolerant of a large excess of borohydride in the aqueous phase and did not decompose, suggesting that charging of the metal core by direct access of the reducing agent through voids in the ligand shell was no longer possible.

Characterization. The purified MPCs obtained as dark-brown solids were subjected to a number of complementary analytical techniques typically employed for the characterization of such materials. UV−vis spectroscopy gives the typical featureless spectra indicative of particles with a core diameter below 3 nm showing in the UV range strongly increasing absorption with decreasing wavelength due to d-band transitions, while a plasmon band is absent (see Supporting Information). Figure 1 shows the FTIR spectra of mercaptocarborane and that of the corresponding MPCs. The main characteristic bands are labeled in both cases. Strong broad absorptions at 2596−2573 cm^{-1} in both the pure mercaptacarborane and the final product, due to B−H stretches, dominate the IR spectra and support a *closo* cluster structure.[26] In addition, the IR spectrum of MPCs exhibits ν(C−H) stretch absorption at 3063 cm^{-1} confirming the presence of C_c−H bond[27] in the gold nanoparticles. Comparison of the spectra clearly demonstrates that mercaptocarborane is the IR active component of the product.

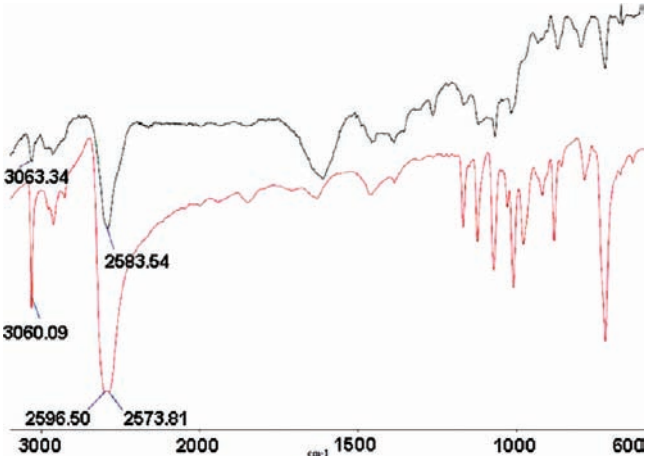

Figure 1. Comparison between the IR spectra of mercaptocarborane (red) and MPCs (black).

The presence of the mercaptocarborane in the ligand shell of the product was further confirmed by ^{1}H and ^{11}B NMR spectroscopy in CD_3COCD_3. The ^{1}H NMR clearly shows the absence of the S−H proton after attachment of the ligand to the gold. Furthermore, the broad single resonance corresponding to C−H bond[22] moves from 4.84 to 4.42 ppm once the ligand coordinates to the gold nanoparticle (see Supporting Information for details). Figure 2 shows a comparison between the ^{11}B NMR spectrum of our MPCs and the NMR spectrum of mercaptocarborane alone. While there are clear differences in the peak patterns indicating a strong interaction between the ligand and the metal core, the range of the chemical shifts fully coincides in both spectra giving further evidence that the *closo* structure is retained in the final product.

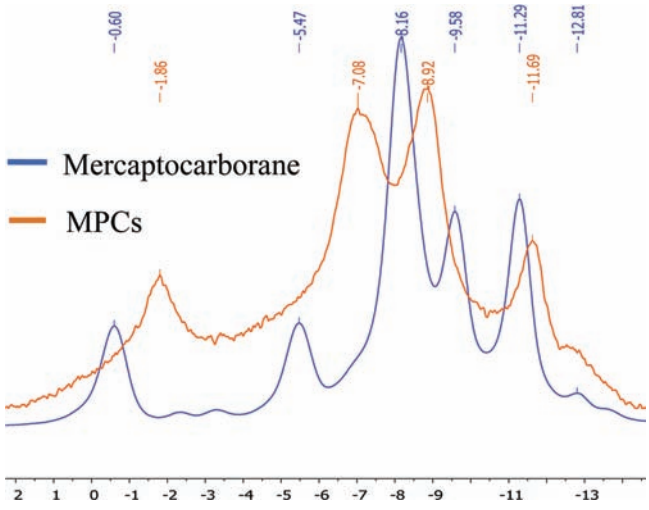

Figure 2. Comparison between ^{11}B NMR spectra of mercaptocarborane and mercaptocarborane attached to Au nanoparticles.

Most notably, the peak at −5.5 ppm in the spectrum of the pristine mercaptocarborane shifts upfield in the MPCs as a result of the gold bonding. This has been reported before for the corresponding carboranylthiolates after coordination to metal, in which the sulfur provides a bridge to transfer electron density from the rich transition metal to the electron-deficient carborane cage.[28] Thus, the carborane electron density in the MPCs is higher than in the parent thiol.

Particle Size. HAADF images of the particles at lower and higher magnification and the corresponding distribution of Au-core sizes are shown in Figure 3. The mean core diameter of 1.1 nm suggests that the well-known Au_{102} cluster is present as the majority species in this preparation. A series of smaller clusters is also present, down at the limit to a very small fraction of species that contain just a single gold atom (see Figure 3b). Some of these atomically dispersed species are artifacts arising from electron beam damage of larger particles, but the majority are genuine components of the sample. The inability to obtain crisp lattice images of the particles is due to their very small size, high mobility (rolling and reorientation), and temporary loss of crystallinity (melting) under the electron beam (see Figure S7, Supporting Information). In contrast, more distinct high-resolution images are obtained from larger particles of 3−7 nm core diameter, which are very occasionally found as a minority species in this material (see Figure S8, Supporting Information). The carborane ligand shell, unsurprisingly, is not visible against the backgound contrast of the carbon support film.

In the UV−vis spectrum of the material the absence of a plasmon band confirms that the typical gold core size is below 3 nm (see Supporting Information). As presented in Figure 4, a mean particle size including the ligand shell of 3.2 nm was estimated by centrifugal particle sizing (CPS), a technique that reaches its limitation at the 5 nm and below range. Taking into account the known diameter of the carborane cage of near 0.5 nm,[29] a mean total particle diameter of 2.1 nm would be expected based on the STEM results.

Partial elemental analysis was also carried out for Au and B by ICP-AES and for Au, B, and S by XPS. By ICP-AES a Au:B molar ratio of 1:6.5 was found and by XPS a Au:B:S relative

dx.doi.org/10.1021/ja203367h | J. Am. Chem.Soc. 2012, 134, 212−221

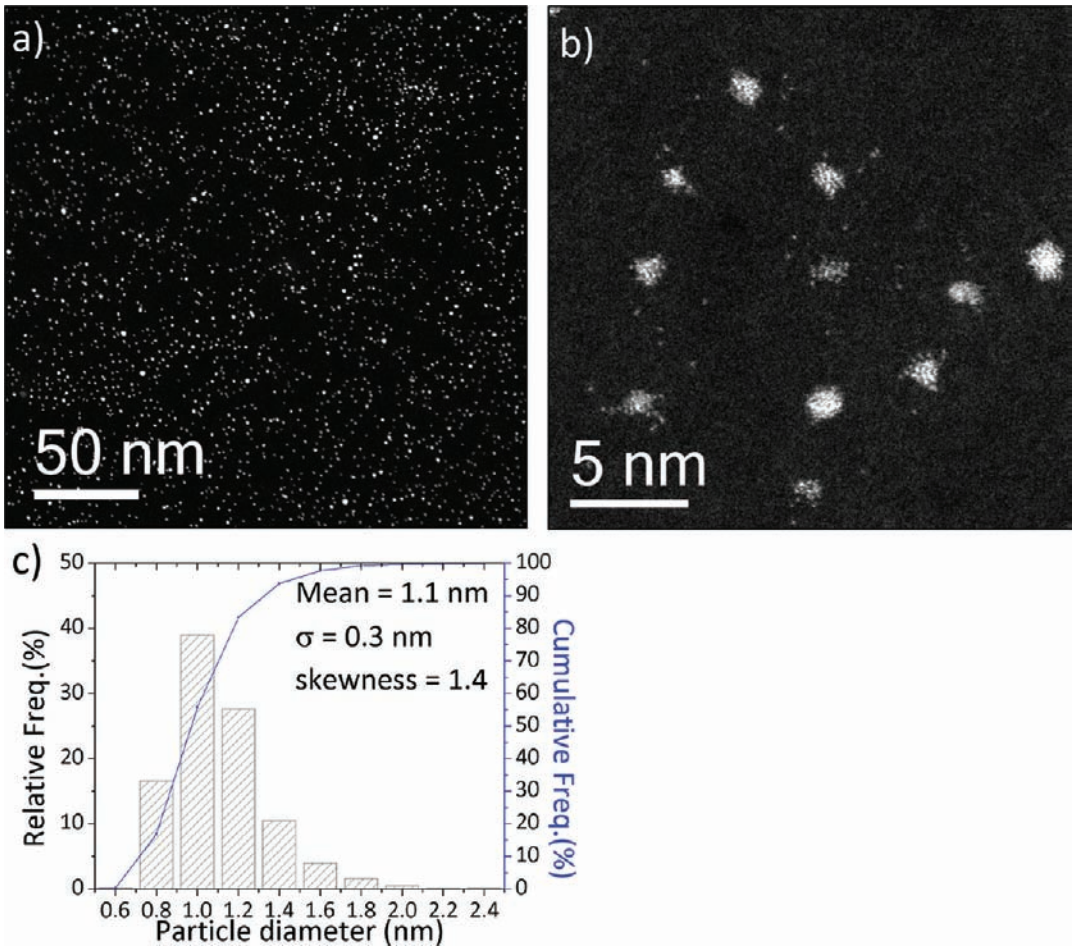

Figure 3. Representative (a) low- and (b) high-magnification STEM-HAADF images of the Au particles supported on a continuous carbon film. (c) Corresponding particle size distribution derived from measurements on ~2000 particles. Notice that species containing single Au atoms can be seen as bright dots in (b).

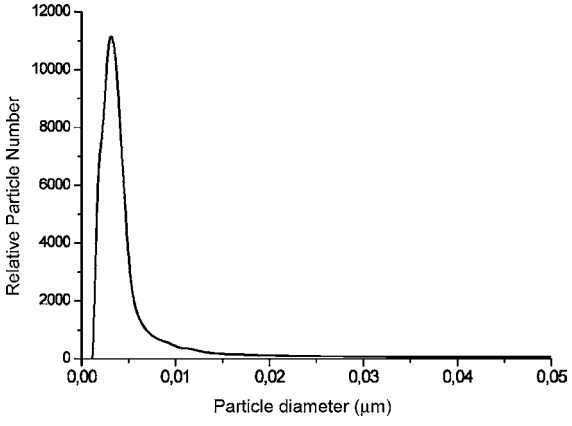

Figure 4. Size distribution of MPCs determined by analytical centrifugation at 24 000 rpm rotation speed, showing a mean particle diameter of 3.2 nm.

molar content of 2.17:16.15:1.31 was obtained. TGA gave a weight loss attributable to the loss of mercaptocarborane ligands of 31.93%. These results are all in good agreement with each other and indicate an average proportion of 0.6 ligand molecules per gold atom. This empirical ratio is rather large in comparison to that of well-known MPCs of gold, such as $Au_{102}(SR)_{44}$[9] or $Au_{144}(SR)_{60}$,[30] but can be explained by the minority presence of a significant population of extremely small clusters and even complexes that only contain a single gold atom, probably of the type $Au(SR)_2$, as evidenced by STEM-HAADF images. In addition, mercaptocarboranes differ significantly from the typically used alkanethiols, and it can be argued that they should favor a somewhat higher ligand coverage. Conventional thiols do not exhibit the same acidity, volume, self-organization possibilities, and coordinating character of the sulfur atom nor the same possibility to generate interactions between each other as do mercaptocarboranes.[31] The rigid and globular form of the *ortho*carborane ligand is very different from that of an alkane. Among typical organic ligands, the closest shape to that of the *ortho*carborane cluster would be a rotating benzene moiety,[32] but even in this case, neither the possibility of self-interactions nor the packing efficiency would be comparable. The *ortho*carborane *via* its acidic $C_{cluster}$–H bond gives rise to hydrogen or dihydrogen interactions with neighboring clusters B–H groups ($C_{cluster}$–H···H–B).[33] These interactions are not possible for alkanes. Thus it is not unreasonable to expect a slightly higher packing density of ligands for the mercaptocarborane MPCs in comparison with organic groups, e.g., alkanes. Moreover, the *ortho*carborane attracts electrons through the cluster carbon atoms more readily than benzene.[34] To obtain final certainty about the exact composition of each particle, either high-resolution mass spectra or crystal structures would be needed. Such work is underway.

dx.doi.org/10.1021/ja203367h | J. Am. Chem.Soc. 2012, 134, 212–221

Ion Exchange. To demonstrate the ability of the MPCs to store ionic charge, a sample dissolved in water was passed trough a lithium ion exchange column[36] and subsequently analyzed by ^{7}Li NMR spectroscopy. Using acetone as solvent, a single sharp peak at 2.02 ppm in the ^{7}Li NMR spectrum of the MPCs was observed. This is clearly indicative of the presence of lithium ions in the MPCs. In addition, by comparison with a reference solution of lithium chloride in acetone, the Li resonance in the MPCs is about 1 ppm deshielded (Figure 5).

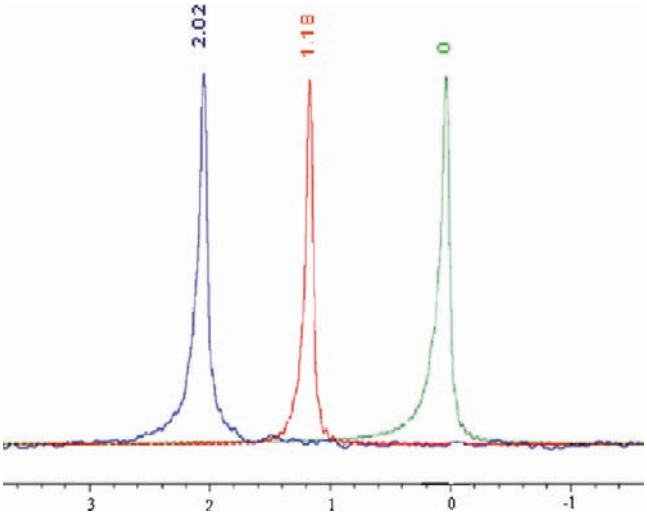

Figure 5. Comparison between ^{7}Li spectra: reference (LiCl 1 M in D_2O) (green), LiCl 1 M in d_6-acetone (red), and MPCs in d_6-acetone (blue).

This evidence that the lithium in MPCs is not so thoroughly solvated by acetone as it is in the case of lithium chloride in the same solvent and that lithium ions polarize electron density from its surroundings, either from the gold nanoparticle or the hydrogen B−H vertexes, that possess a partial hydride character or both.

Note that in aqueous medium sodium ions are strongly associated with the MPCs and are probably located in the voids between adjacent mercaptoborane cages. In the exchange column, they are replaced stoichiometrically by lithium ions, which are now sitting inside the voids in contact with or close proximity to the gold surface.

Cellular Uptake and Intracellular Fate. These preliminary experiments were conducted to investigate how our hydrophilic MPCs, that have the unique property of becoming hydrophobic when oxidized, interact with biological cells. This is of interest since a cell represents a medium that is strongly compartmentalized into aqueous microenvironments separated from each other by hydrophobic membrane barriers. Our expectation was that the MPCs can cross these barriers easier than purely hydrophilic particles and that they eventually end up as hydrophobic inclusions in membranes. Although the intracellular environment is generally described as reductive, it should be oxidative with respect to the MPCs that have been prepared in the presence of a high concentration of sodium borohydride. The results discussed below suggest that this is indeed the case. For this study, we chose HeLa cells, a common human fibroblast cell line, which has frequently been used to investigate cellular uptake of nanoparticles. The first clear difference compared to standard gold nanoparticles is that our MPCs are relatively toxic so that all cells died after 24 h of incubation with them. We therefore restricted the time the cells were in contact with the particles to 2 h. Under these conditions the cells remained alive even 48 h after they had been incubated. TEM images of cell sections prepared immediately after the 2 h incubation time are shown in Figure 6.

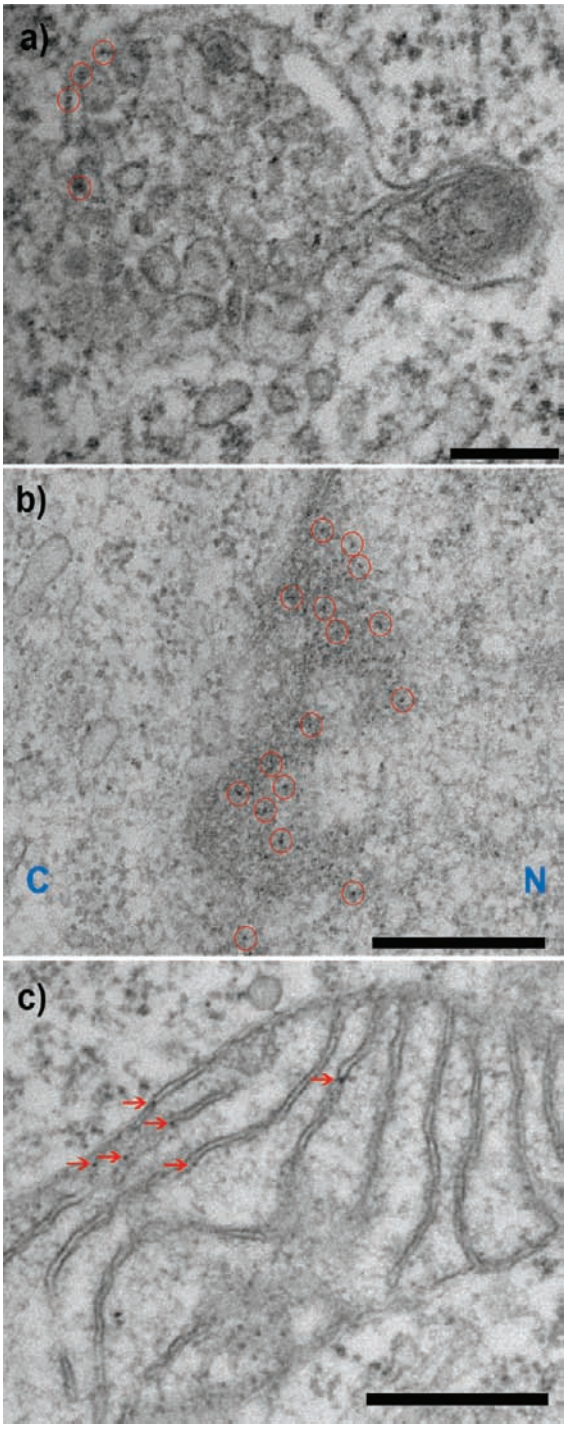

Figure 6. MPCs after uptake by HeLa cells, precipitated into the membranes of a multivesicular body (a), in the nuclear envelope (b), and in the mitochondria (c). Red circles and arrows have been added for clarity. Scale bars are 200 nm.

As expected, the particles are very small, and it is probably not possible to identify individual ones in these images. Nevertheless, aggregates composed of several particles can be clearly

distinguished. It is a general problem with standard TEM imaging of intracellular metal particles below about 5 nm that these are often indistinguishable from stained proteins and other subcellular structures of comparable size. As Supporting Information, we have therefore added for comparison similar images obtained in the absence of MPCs to demonstrate that the excellent contrast provided by the gold, in this case does indeed provide us with confidence to identify and locate aggregates of MPCs, some of which have been labeled for clarity with red circles or arrows. The images in Figure 6 show features belonging to three different compartments, a multivesicular body, the nuclear envelope, and a mitochondrion. In all cases, most of the aggregated particles are clearly identified and reside within membrane structures, which is particularly clear in the case of the nuclear envelope, part of which is densely decorated with aggregates. A number of aggregates are also found in the cytosol and in the nucleus. These findings support the hypothesis that the particles are initially dispersed in the aqueous phase of the cell, where they appear to be able to diffuse freely into various organelles, and then gradually become oxidized and rendered hydrophobic, which leads to aggregation followed by precipitation of the aggregates into membrane structures. To confirm the involvement of redox processes in this behavior, we have investigated the formation of ROS, which include OH radicals formed as a consequence of enhanced redox activity within the cell. The confocal microscopy image in Figure 7

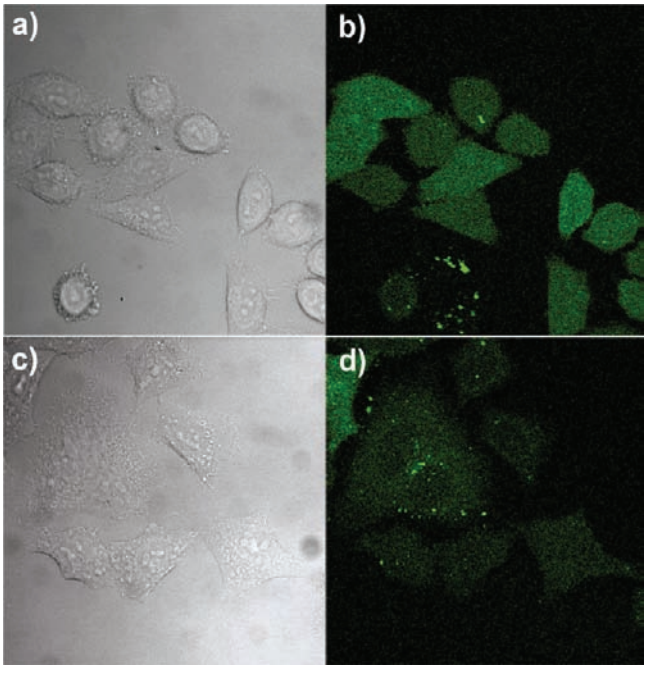

Figure 7. Confocal microscopy: incubation with MPCs causes oxidative stress. ROS monitored by the appearance of green fluorescence: (a, b) HeLa cells incubated MPCs nanoparticles for 30 min and (c, d) same as (a) but in the absence of gold nanoparticles.

clearly shows significantly enhanced ROS levels after incubation with MPCs, indicating the formation of radicals and subsequent oxidative stress that we attribute to the loss of electrons (and sodium ions) from the MPCs, as shown in Scheme 2.

The behavior of our MPCs in the biological environment is highly unusual and further confirms that these particles have properties that differ significantly from those of standard preparations. Most commonly, nanoparticles are taken up by endocytosis and are not able to transfer spontaneously across membrane boundaries.[37] They tend to remain confined to endocytic vesicles, such as those shown in Figure 6a, and do not reach the cytoplasm or the nucleus and least of all the mitochondria, which have no mechanisms for the direct uptake of particular matter and, like the nucleus, are surrounded by a double membrane. The toxicity of these new MPCs and their ability to readily reach intracellular targets makes them attractive candidates for further studies in view of potential anticancer activity or as boron-rich agents for BNCT. The above observations together suggest that in this system, ligand exchange with intracellular glutathione, as reported by Rotello and coworkers,[13b] within the time scale of our experiments only plays a minor role, if any, since it would render the particles hydrophilic and prevent their precipitation into membrane structures. Resisting ligand exchange is quite common and has been observed before for particles stabilized with peptides and/or polyethylene glycol-based ligands.[17a,f] To what extent our particles do undergo chemical modifications inside the cell remains to be studied in future work.

■ CONCLUSIONS AND OUTLOOK

A new MPC system has been introduced showing very unusual redox switchable solubility properties that are due to the metallic core and the designed openness and thinness of the ligand shell consisting of carborane clusters. This allows the particle to store electronic charge in the core and ionic charge in the ligand shell in Nernstian equilibrium with its environment.

A simple structural and functional model has been proposed that explains all observed phenomena and is fully consistent with the compositional and spectroscopic characterization of the material. Uptake of the particles by a human cancer cell line has been demonstrated, and their intracellular fate was investigated by electron microscopy, showing the preferential location of the particles in vesicles within membranes and in the nucleus. Unlike most other preparations of gold nanoparticles, these particles are toxic and eventually lead to cell death presumably resulting from their high reducing power that leads to the formation of free radicals. These new MPCs display a host of fascinating properties that suggest applications in catalysis and electrocatalysis and the possibility of new nanoscopic electron and ion valves to be integrated in artificial and biological membranes. In addition, new electrochemical sensors and diagnostic tools may arise from such nanoparticles. The material should also be attractive as a boron-rich agent for BNCT. Finally, there is now a need for a thorough electrochemical characterization of the particles to quantify their charge storage ability and to unravel the precise mechanisms of electronic and ionic charging.

■ ASSOCIATED CONTENT

Ⓢ Supporting Information

Movie illustrating the transfer of MPCs from aqueous solution to ether phase upon addition of *tetra*octylammonium bromide. Comparison between IR spectra of 1-octanethiol and of MPCs before and after addition of 1-octanethiol. ^{1}H NMR spectra of mercaptocarborane and MPCs. UV−vis (300−800 nm) of MPCs in isopropanol. TGA and DSC as well as TEM images of HeLa cells in the absence of MPCs compared to those containing MPCs. Additional STEM-HAADF micrographs showing particle stability effects and occasional larger, more crystalline Au particles. This material is available free of charge via the Internet at http://pubs.acs.org.

dx.doi.org/10.1021/ja203367h | *J. Am. Chem.Soc.* 2012, 134, 212−221

AUTHOR INFORMATION

Corresponding Author
clara@icmab.es; m.brust@liv.ac.uk

ACKNOWLEDGMENTS

This research has been financed by MEC (CTQ2010-16237) and Generalitat de Catalunya (2009/SGR/00279). Ana M. Cioran and Ana D. Musteti are enrolled in the PhD program of the UAB and they also thank MEC for FPU predoctoral grants.

REFERENCES

(1) (a) Brust, M.; Walker, M.; Bethell, D.; Schiffrin, D. J. *J. Chem. Soc. Chem. Commun.* **1994**, *7*, 801−802. (b) Brust, M.; Fink, J.; Bethell, D.; Schiffrin, D. J.; Kiely, C. *J. Chem. Soc. Chem. Commun.* **1995**, *16*, 1655−1656. (c) Terrill, R. H.; Postlethwaite, T. A.; Chen, C. H.; Poon, C. D.; Terziz, A.; Chen, A. D.; Hutchison, J. E.; Clark, M. R.; Wignall, G.; Londono, J. D.; Superfine, R.; Falvo, M.; Johnson, C. S.; Samulski, E. T.; Murray, R. W. *J. Am. Chem. Soc.* **1995**, *117*, 12537−12548. (d) Badia, A.; Singh, S.; Demers, L.; Cuccia, L.; Brown, G. R.; Lennox, R. B. *Chem−Eur. J.* **1996**, *2*, 359−362. (e) Hostetler, M. J.; Stokes, J. J.; Murray, R. W. *Langmuir* **1996**, *12*, 3604−3612. (f) Daniel, M. C.; Astruc, D. *Chem. Rev.* **2004**, *104*, 293−346. (g) Boisselier, E.; Astruc, D. *Chem. Soc. Rev.* **2009**, *38*, 1759−1782. (h) Sardar, R.; Funston, A. M.; Mulvaney, P.; Murray, R. W. *Langmuir* **2009**, *25*, 13840−13851.

(2) (a) Ingam, R. S.; Hostetler, M. J.; Murray, R. W.; Schaaf, T. G.; Khoury, J. T.; Whetten, R. L.; Bigioni, T. P.; Guthrie, D. K.; First, P. N. *J. Am. Chem. Soc.* **1997**, *119*, 9279−9280. (b) Chen, S. W.; Ingram, R. S.; Hostetler, M. J.; Pietron, J. J.; Murray, R. W.; Schaaf, T. G.; Khoury, J. T.; Alvarez, M. M.; Whetten, R. L. *Science* **1998**, *220*, 2098−2101. (c) Hicks, J. F.; Templeton, A. C.; Chen, S. W.; Sheran, K. M.; Jasti, R.; Murray, R. W.; Debord, J.; Schaaf, T. G.; Whetten, R. L. *Anal. Chem.* **1999**, *71*, 3703−3711. (d) Quinn, B. M.; Liljeroth, P.; Ruiz, V.; Laaksonen, T.; Kontturi, K. *J. Am. Chem. Soc.* **2003**, *125*, 6644−6645.

(3) (a) Persson, S. H. M.; Olofsson, L.; Gunnarson, L. *App. Phys. Lett.* **1999**, *17*, 2564−2548. (b) Bigioni, T. P.; Harrell, L. E.; Cullen, W. G.; Guthrie, D. E.; Whetten, R. L.; First, P. N. *European Physical Journal D* **1999**, *6*, 355−364. (c) Kano, S.; Azuma, Y.; Kanehara, M.; Teranishi, T.; Majima, Y. *App. Phys. Lett.* **2010**, 10, article number 105003.

(4) (a) Brust, M.; Bethell, D.; Schiffrin, D. J.; Kiely, C. J. *Adv. Mater.* **1995**, *7*, 795−797. (b) Hicks, J. F.; Zamborini, F. P.; Osisek, A.; Murray, R. W. *J. Am. Chem. Soc.* **2001**, *123*, 7048−7053. (c) Fishelson, N.; Shkrob, I.; Lev, O.; Gun, J.; Modestov, A. D. *Langmuir* **2001**, *17*, 403−412. (d) Pelka, J. B.; Brust, M.; Gierlowski, P.; Paszkowicz, W.; Schell, N. *App. Phys. Lett.* **2006**, 89, article number 063110.

(5) (a) Whetten, R. L.; Khoury, J. T.; Alvarez, M. M.; Murthy, S.; Vezmar, I.; Wang, Z. L.; Stephens, P. W.; Cleveland, C. L.; Luedke, W. D.; Landman, U. *Adv. Mater.* **1996**, *8*, 428−433. (b) Kiely, C. J.; Fink, J.; Brust, M.; Schiffrin, D. J.; Bethell, D. *Nature* **1998**, *396*, 144−146. (c) Kiely, C. J.; Fink, J.; Zheng, J. G.; Brust, M.; Schiffrin, D. J. *Adv. Mater.* **2000**, *12*, 640−643. (d) Stoeva, S. I.; Prasad, B. L. V.; Uma, S.; Stoimenov, P. K.; Zaikovski, V.; Sorensen, C. M.; Klabunde, K. L. *J. Phys. Chem. B* **2003**, *107*, 7441−7448. (e) Courty, A.; Mermet, A.; Albouy, P. A.; Duval, E.; Pileni, M. P. *Nat. Mater.* **2005**, *4*, 395−398. (f) Bigioni, T. P.; Lin, X. M.; Nguyen, T. T.; Corwin, E. I.; Witten, T. A.; Jaeger, H. M. *Nat. Mater.* **2006**, *5*, 265−270. (g) Prasad, B. L. V.; Sorensen, C. M.; Klabunde, K. J. *Chem. Soc. Rev.* **2008**, *37*, 1871−1883.

(6) (a) Collier, C. P.; Saykally, R. J.; Shiang, J. J.; Henrichs, S. E.; Heath, J. R. *Science* **1998**, *277*, 1978−1981. (b) Quinn, B. M.; Prieto, I.; Haram, S. K.; Bard, A. J. *J. Phys. Chem. B* **2001**, *105*, 7474−7476.

(7) (a) Badia, A.; Gao, W.; Singh, S.; Demers, L.; Cuccia, L.; Reven, L. *Langmuir* **1996**, *12*, 1262−1269. (b) Badia, A.; Demers, L.; Dickinson, L.; Morin, F. G.; Lennox, R. B.; Reven, L. *J. Am. Chem. Soc.* **1997**, *119*, 11104−11105. (c) Templeton, A. C.; Cliffel, D. E.; Murray, R. W. *J. Am. Chem. Soc.* **1999**, *121*, 7081−7089. (d) Badia, A.; Lennox, R. B.; Reven, L. *Acc. Chem. Res.* **2000**, *33*, 475−481. (e) Donkers, R. L.; Song, Y.; Murray, R. W. *Langmuir* **2004**, *20*, 4703−4707.

(8) (a) Wohltjen, H.; Snow, A. W. *Anal. Chem.* **1998**, *70*, 2856−2859. (b) Joseph, Y.; Peic, A.; Chen, X. D.; Michl, J.; Vossmeyer, T.; Yasuda, A. *J. Phys. Chem. C* **2007**, *111*, 12855−12859. (c) Barash, O.; Peled, N.; Hirsch, F. R.; Haick, H. *Small* **2009**, *5*, 2618−2624. (d) Peng, G.; Tisch, U.; Adams, O.; Hakim, M.; Shehada, N.; Broza, Y. Y.; Billan, S.; Abdah-Bortnyak, R.; Kuten, A.; Haick, H. *Nat. Nanotechnol.* **2009**, *4*, 669−673. (e) Chow, E.; Gengenbach, T. R.; Wieczorek, L.; Raguse, B. *Sens. Actuators, B* **2010**, *143*, 704−711. (f) Covincton, E.; Bohrer, F. I.; Xu, C.; Zellers, E. T.; Kurdak, C. *Lab Chip* **2010**, *22*, 3058−3060.

(9) Jadzinsky, P. D.; Calero, G.; Ackerson, C. D.; Bushnell, D. A.; Kornberg, R. D. *Science* **2007**, *318*, 430−433.

(10) (a) Wen, F.; Englert, U.; Gutrat, B.; Simon, U. *Eur. J. Inorg. Chem.* **2008**, *1*, 106−111. (b) Zhu, M.; Aikens, C. M.; Hollander, F. J.; Schatz, G. C.; Jin, R. *J. Am. Chem. Soc.* **2008**, *130*, 5883−5885. (c) Qian, H. F.; Eckenhoff, W. T.; Zhu, Y.; Pintauer, T.; Jin, R. C. *J. Am. Chem. Soc.* **2010**, *132*, 8280−8281. (d) Parker, J. F.; Fields-Zinna, C. A.; Murray, R. W. *Acc. Chem. Res.* **2010**, *43*, 1289−1296.

(11) (a) Akola, J.; Walter, M.; Whetten, R. L.; Hakkinen, H.; Gronbeck, H. *J. Am. Chem. Soc.* **2008**, *130*, 3756−3757. (b) Walter, M.; Akola, J.; Lopez-Acevedo, O.; Jadzinsky, P. D.; Calero, G.; Ackerson, C. J.; Whetten, R. L.; Gronbeck, H.; Hakkinen, H. *Proc. Natl. Acad. Sci. U.S.A.* **2008**, *105*, 9157−9162. (c) Jiang, D. E.; Walter, M.; Akola, J. J. *Phys. Chem. C* **2010**, *114*, 15883−15889. (d) Aitkens, C. M. J. *Phys. Chem. Lett.* **2010**, *2*, 99−104.

(12) Pedersen, J.; Bjornholm, S.; Borggreen, J.; Hansen, K.; Martin, T. P.; Rasmussen, H. D. *Nature* **1991**, *353*, 733−735.

(13) (a) Paciotti, G. F.; Myer, L.; Weinreich, D.; Goia, D.; Pavel, N.; McLaughlin, R. E.; Tamarkin, L. *Drug Delivery* **2004**, *11*, 169−183. (b) Hong, R.; Han, G.; Fernandez, J. M.; Kim, B. J.; Forbes, N. S.; Rotello, V. M. *J. Am. Chem. Soc.* **2006**, *128*, 1078−1079. (c) Chithrani, B. D.; Chan, W. C. W. *Nano Lett.* **2007**, *7*, 1542−1550. (d) Podsiadlo, P.; Sinani, V. A.; Bahng, J. H.; Kam, N. W. S.; Lee, J.; Kotov., N. A. *Langmuir* **2008**, *24*, 568−574. (e) Ghosh, P. S.; Kim, C. K.; Han, G.; Forbes, N. S.; Rotello, V. M. *ACS Nano* **2008**, *2*, 2213−2218. (f) Kim, C.; Agasti, S. S.; Zhu, Z. J.; Isaacs, L.; Rotello, V. M. *Nat. Chem.* **2010**, *2*, 962−966. (g) Krpetic, Z.; Nativo, P.; See, V.; Prior, I. A.; Brust, M.; Volk, M. *Nano Lett.* **2010**, *10*, 4549−4554. (h) Gil- Tomas, J.; Dekker, L.; Narband, N.; Parkin, I. P.; Nair, S. P.; Street, C.; Wilson, M. *J. Mater. Chem.* **2011**, *21*, 4189−4196.

(14) (a) de la Fuente, J. M.; Barrientos, A. G.; Rojas, T. C.; Rojo, J.; Fernandez, A.; Penades, S. *Angew. Chem., Int. Ed.* **2001**, *40*, 2258−2261. (b) Barrientos, A. G.; de la Fuente, J. M.; Rojas, T. C.; Fernandez, A.; Penades, S. *Chem.—Eur. J.* **2003**, *9*, 1909−1921. (c) Rojo, J.; Diaz, V.; de la Fuente, J. M.; Segura, I.; Barrientos, A. G.; Riese, H. H.; Bernade, A.; Penades, S. *ChemBioChem* **2004**, *5*, 291−297. (d) Garcia, I.; Marradi, M.; Penades, S. *Nanomedicine* **2010**, *5*, 777−792.

(15) (a) Levy, R.; Thanh, N. T. K.; Doty, R. C.; Hussain, I.; Nichols, R.; Schiffrin, D. J.; Brust, M.; Fernig, D. G. *J. Am. Chem. Soc.* **2004**, *126*, 10076−10084. (b) Pengo, P.; Polizzi, S.; Pasquato, L.; Scrimin, P. *J. Am. Chem. Soc.* **2005**, *127*, 1616−1617. (c) Slocik, J. M.; Stone, M. O.; Naik, R. R. *Small* **2005**, *1*, 1048−1052. (d) Levy, R. *ChemBioChem* **2006**, *7*, 1145−1145. (e) Pengo, P.; Baltzer, L.; Pasquato, L.; Scrimin, P. *Angew. Chem., Int. Ed.* **2007**, *46*, 400−404. (f) Krpetic, Z.; Nativo, P.; Porta, F.; Brust, M. *Bioconjugate Chem.* **2009**, *20*, 1619−1624.

(16) (a) Hussain, I.; Graham, S.; Wang, Z. X.; Tan, B.; Sherrington, D. C.; Rannard, S. P.; Cooper, A. I.; Brust, M. *J. Am. Chem. Soc.* **2005**, *127*, 16398−16399. (b) Wang, Z. X.; Tan, B. E.; Hussain, I.; Schaeffer, N.; Wyatt, M. F.; Brust, M.; Cooper, A. I. *Langmuir* **2007**, *23*, 885−895.

(17) (a) Wuelfing, W. P.; Gross, S. M.; Miles, D. T.; Murray, R. W. *J. Am. Chem. Soc.* **1998**, *120*, 12696−12697. (b) Bartz, M.; Kuther, J.; Nelles, G.; Weber, N.; Seshadri, R.; Tremel, W. *J. Mater. Chem.* **1999**, *9*, 121−1125. (c) Kanaras, A. G.; Kamounah, F. S.; Schaumburg, K.; Kiely, C. J.; Brust, M. *Chem. Commun.* **2002**, *20*, 2294−2295. (d) Ishii, T.; Otsuka, H.; Kataoka, K.; Nagasaki, Y. *Langmuir* **2004**, *20*, 561−564. (e) Tshikhudo, T. R.; Demuru, D.; Wang, Z. X.; Brust, M.; Secchi, A.; Arduini, A.; Pochini, A. *Angew. Chem., Int. Ed.* **2005**, *44*,

2913−2916. (f) Duchesne, L.; Gentili, D.; Comes-Franchini, M.; Fernig, D. G. *Langmuir* **2008**, *24*, 13572−13580.
(18) Quinn, B. M.; Kontturi, K. *J. Am. Chem. Soc.* **2004**, *126*, 7168−7169.
(19) (a) Henglein, A.; Lilie, J. *J. Am. Chem. Soc.* **1981**, *103*, 1059−1066. (b) Henglein, A. *Top. Curr. Chem.* **1988**, *143*, 113−180. (c) Henglein, A. *Chem. Rev.* **1989**, *89*, 1861−1873.
(20) Grimes, R. N. *Carboranes*; Academic Press: New York, 1970.
(21) (a) Hawthorne, M. F.; Maderna, A. *Chem. Rev.* **1999**, *99*, 3421−3434. (b) Barth, R. F.; Coderre, J. A.; Vicente, M. G. H.; Blue, T. E. *Clin. Cancer Res.* **2005**, *11*, 3987−4002. (c) Gottumukkala, V.; Ongayi, O.; Baker, D. G.; Lomax, L. G.; Vicente, M. G. H. *Bioorg. Med. Chem.* **2006**, *14*, 1871−1879. (d) Wang, J.-Q.; Ren, C.-X.; Weng, L.-H.; Jin, G.-X. *Chem. Commun.* **2006**, 162−164. (e) Bregadze, V. I.; Sivaev, I. B.; Glazun, S. A. *Anti-Cancer Agents Med. Chem.* **2006**, *6*, 75−109.
(22) (a) Smith, H. D.; Obenland, C. O.; Papetti, S. *Inorg. Chem.* **1966**, *5*, 1013. (b) Viñas, C.; Benakki, R.; Teixidor, F.; Casabó. *J. Inorg. Chem* **1995**, *34*, 3844−3845.
(23) Baše, T; Bastl, Z; Plzák, Z.; Grygar, T; Plešek, J.; Carr, M. J.; Malina, V.; Šubrt, J.; Bohácek, J.; Vecerníková, E.; Kříž, O. *Langmuir* **2005**, *21*, 7776−7785.
(24) Kennedy., D. C.; Duguay, D. R.; Tay, L.-L.; Richeson, D. S.; Pezacki, J. P. *Chem. Commun.* **2009**, 6750−6752.
(25) (a) Hohman, J. N.; Claridge, S. A.; Kim, M.; Weiss, P. S. *Mater. Sci. Eng., R* **2010**, *70*, 188−208. (b) Baše, T; Bastl, Z; Havránekc, V.; Langa, K.; Bould, J.; Londesborough, M. G. S.; Macháček, J.; Plešek, J. *Surf. Coat. Technol.* **2010**, *204*, 2639−2646. (c) Hohman, J. N.; Zhang, P.; Morin, E. I.; Han, P.; Kim, M.; Kurland, A. R.; McClanahan, P. D.; Balema, V. P.; Weiss, P. S. *ACS Nano* **2009**, *3*, 527−536.
(26) Leites, L. A. *Chem. Rev.* **1992**, *92*, 279−323.
(27) Leites, L. A.; Vinogradova, L. E. *J. Organomet. Chem.* **1977**, *125*, 37−41.
(28) (a) Teixidor, F.; Viñas, C.; Sillanpää, R.; Kivekäs, R. *Inorg. Chem.* **1994**, *33*, 2645. (b) Teixidor, F.; Pedradas, J.; Viñas, C. *Inorg. Chem.* **1995**, *34*, 1726. (c) Kivekäs, R.; Sillanpää, R.; Teixidor, F.; Viñas, C.; Núñez, R. *Acta Crystallogr., Sect. C* **1994**, *50*, 2027. (d) Llop, J.; Viñas, C.; Oliva, J. M.; Teixidor, F.; Flores, M. A.; Kivekäs, R.; Sillanpää, R. *J. Organomet. Chem.* **2002**, *657*, 232. (e) Oliva, J. M.; Allan, N. L.; Schleyer, P. V.; Viñas, C; Teixidor, F *J. Am. Chem. Soc.* **2005**, *127* (39), 13538−13547.
(29) Kivekäs, B.; Benakki, R.; Viñas, C.; Sillanpää, R. *Acta Crystallogr.* **1999**, *C55*, 1581−1583.
(30) Lopez-Acevedo, O.; Akola, J.; Whetten, R. L.; Grönbeck, H.; Häkkinen, H. *J. Phys. Chem. C* **2009**, *113* (13), 5035−5038.
(31) (a) Batsanov, A. S.; Fox, M. A.; Hibbert, T. G.; Howard, J. A. K.; Kivekäs, R.; Laromaine, A.; Sillanpää, R.; Viñas, C.; Wadea, K. *Dalton Trans.* **2004**, 3822−3828. (b) Planas, J. G.; Viñas, C.; Teixidor, F.; Comas-Vives, A.; Ujaque, G.; Lledós, A.; Light, M. E.; Hursthouse, M. B. *J. Am. Chem. Soc.* **2005**, *127*, 15976−15982.
(32) Teixidor, F.; Viñas, C.; Demonceau, A.; Nuñez, R. *Pure Appl. Chem.* **2003**, *75*, 1305−1313.
(33) Puga, A. V.; Teixidor, F.; Sillanpää, R.; Kivekäs, R.; Viñas, C. *Chem.—Eur. J.* **2009**, *15*, 9764 −9772.
(34) (a) Núñez, R.; Farràs, P.; Teixidor, F.; Viñas, C.; Sillanpää, R.; Kivekäs, R. *Angew. Chem., Int. Ed.* **2006**, *45*, 1270 −1272. (b) Teixidor, F.; Núñez, R.; Viñas, C.; Sillanpää, R.; Kivekäs, R. *Angew. Chem. Int. Ed* **2000**, *39*, 4290 −4292.
(35) Artigas, M. M.; Crespo, O.; Gimeno, M. C.; Jones, P. G.; Laguna, A.; Villacampa, M. D. *J. Organomet. Chem.* **1998**, *561* (1−2), 1−6.
(36) Cation exchange resin strongly acidic PA (provided by Panreac) with a total exchange capacity of 2.0 meq/mL and a water content of 46−52%, loaded with lithium chloride.
(37) Brandenberger, C.; Muhlfeld, C.; Ali, Z.; Lenz, A. G.; Schmid, O.; Parak, W. J.; Gehr, P.; Rothen-Rutishauser, B. *Small* **2010**, *6*, 1669−1678.